
Journal of Computer-Aided Materials Design, **8:** 233–243, 2001.
KLUWER/ESCOM

Viscosities of liquid metal alloys from nonequilibrium molecular dynamics

YUE QI, TAHIR ÇAĞIN*, YOSHITAKA KIMURA and WILLIAM A. GODDARD III
Materials and Process Simulation Center, Beckman Institute (139-74) Division of Chemistry and Chemical Engineering, California Institute of Technology, Pasadena, CA 91125, U.S.A.

Received 1 October 2001; Accepted 28 October 2001

Abstract. We have developed a nonequilibrium molecular dynamics (NEMD) approach to predict viscosity by including external shear rates directly into the Hamiltonian equations of motion. Using the quantum Sutton–Chen (Q–SC) many-body potentials for Au and Cu, we applied NEMD to predict the viscosity as a function of shear rates for Au_xCu_{1-x} alloys with x ranging from 0 to 100%. This was done for temperatures of 1500 K to 2000 K. The predicted viscosities are in reasonable agreement with experiment. In particular, we find that fixing the density and changing the temperature leads to very little change in the shear viscosity. Thus, the temperature dependence in viscosity is mainly due to the change in density with temperature.

Keywords: Cu-Ag Alloy, Liquid metals, Viscosity

1. Introduction

Reliable data on the viscosity of liquid metals is important for designing and optimizating of metallurgical processes, such as refining, casting, welding, and solidification. Experimental data on viscosity is inadequate for the needs of today's technology. Equations have been proposed to estimate the viscosity of liquid metals based on experimental and theoretical relations (e.g., recent work by Hirai [1] and Seetharaman [2]) but these equations may not provide adequate accuracy.

Our objective is to provide a bridge between experiment and theory by providing a sound foundation for molecularly based theories of rheology. The nonequilibrium molecular dynamics (NEMD) technique enables us to determine the transport coefficients from the response of the system to finite applied fields [3, 4]. In NEMD, the viscosity is calculated in the same way that an experimentalist would measure it. The shear viscosity coefficient η is obtained directly by evaluating the momentum flux in a system subject to a known applied shear rate $\dot{\gamma}$. NEMD can evaluate the pressure and viscometic function in addition to the shear viscosity, enabling us to study the fluid microstructure in the nonequilibrium steady state.

NEMD methods have been used to study many systems, such as molten NaCl [5], N-alkanes [6, 7], water [8], liquid crystals [9], etc. In this paper we applied NEMD to calculate the shear viscosity of Cu-Au alloys (applying planar Couette shear flow).

We used the quantum Sutton–Chen (Q–SC) many-body force field (FF)[10–12]. The parameters were optimized for Cu and Au by fitting to such experimental properties as density, cohesive energy, moduli, and phonon frequencies [12]. The parameters for the alloys are obtained using combination rules. These parameters lead to accurate values for surface energies,

*To whom correspondence should be addressed. E-mail: tahir@wag.caltech.edu

vacancies energies, and stacking faults energy. Consequently, we expect these to be accurate for describing shear flow.

Section 2 describes the methodology, while Section 3 discusses the results.

2. Calculational methods

2.1. Interaction potential and parameters

The Q–SC many-body FF describes the total potential energy of the metal as

$$U_{\text{tot}} = \sum_i U_i = \sum_i \left[\sum_{i \neq j} D_{ij} \frac{1}{2} V\left(r_{ij}\right) - c_i D_i i \rho_{ij}^{1/2} \right], \tag{1}$$

where r_{ij} is the distance between atoms i and j, $V(r_{ij})$ is a pairwise potential

$$V\left(r_{ij}\right) = \left[\frac{\alpha_{ij}}{r_{ij}} \right]^{n_{ij}} \tag{2}$$

(accounting for the short-range repulsion) between the cores of atoms i and j, and ρ_i is a local density associated with atom i and defined as

$$\rho_{ij} = \sum_{j \neq i} \phi\left(r_{ij}\right) = \sum_{j \neq i} D_{ij} \left(\frac{\alpha_{ij}}{r_{ij}} \right)^{m_{ij}}. \tag{3}$$

This term describes the attractive forces of metallic bonding. The sums in Eq. 1 are for $r_{ij} < 2\alpha_{ij}$ (a cutoff of twice of the cubic lattice parameter of the material).

In the above equations, D sets the overall energy scale, while c is a dimensionless parameter scaling the attractive metallic bonding term relative to the Pauli repulsive term. α is a length parameter leading to a dimensionless form for V and ρ. To extend the Q–SC model potentials to alloys, we used the following combination rules to represent the interaction between a Au-Cu pair

$$D_{ij} = \sqrt{D_i D_j} \tag{4}$$

$$m_{ij} = \frac{\left(m_i + m_j\right)}{2}, \tag{5}$$

$$n_{ij} = \frac{\left(n_i + n_j\right)}{2}, \tag{6}$$

$$\alpha_{ij} = \frac{\left(\alpha_i + \alpha_j\right)}{2}. \tag{7}$$

The parameters used in this simulation are shown in Table 1. These Q–SC parameters were obtained by fitting the density, cohesive energy, elastic constant, and phonon dispersion curves. They lead to accurate values for surface energies, vacancy energy, and stacking fault energy. We refer to this modified set of SC parameters as the Q–SC FF.

Table 1. Quantum Sutton–Chen (Q–SC) force field parameters [1]

	D (meV)	c	m	n	α (Å)
Cu	5.7921	84.843	5	10	3.6030
Au	7.8052	53.581	8	11	4.0651

Table 2. The densities (g/cm^3) we used in simulation coming from Ref. 15

	T (K)	1500	1750	2000
Experiment [15]	Cu	17.085	16.687	16.316
	Cu_3Au_1	10.240	9.960	9.689
	Cu_1Au_1	12.518	12.202	11.900
	Cu_1Au_3	14.812	14.444	14.107
	Au	7.953	7.716	7.481

2.2. Planar Couette flow and the shear viscosity

For computational simplicity, the NEMD calculation on sheared fluids is carried out for a system subject to a planar Couette flow (pure shear), with fixed density and temperature. We consider that the applied shear is in the xy plane and changes linearly in the y direction. The system can be exactly modeled by applying the isokinetic SLLOD equations of motion for a molecular fluid [3, 4].

$$\dot{x}_i = \frac{p_{xi}}{m_i} + \dot{\gamma} y_i, \tag{8}$$

$$\dot{y}_i = \frac{p_{yi}}{m_i}, \tag{9}$$

$$\dot{z}_i = \frac{p_{zi}}{m_i}, \tag{10}$$

$$\dot{p}_{xi} = F_{xi} - \dot{\gamma} p_{y_i} - \tau p_{xi}, \tag{11}$$

$$\dot{p}_{yi} = F_{yi} - \tau p_{yi}, \tag{12}$$

$$\dot{p}_{zi} = F_{zi} - \tau p_{zi}, \tag{13}$$

where γ is the shear rate, or the velocity gradient,

$$\dot{\gamma}(t) = \frac{\partial u_x}{\partial y} \tag{14}$$

and u_x is the velocity in the x direction. Here τ is the Gaussian thermostat variable obtained by solving the constraint equation

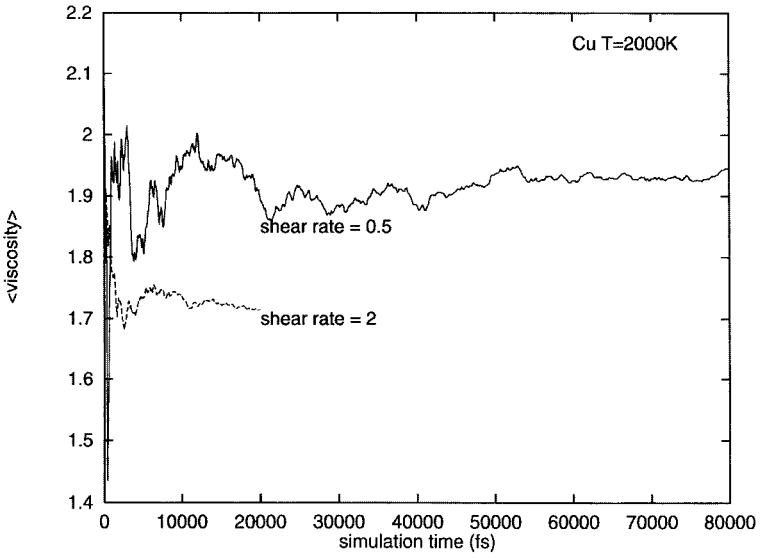

Figure 1. Dependence of calculation viscosity on length of NEMD simulation. For shear rates of 2/ps and 0.5/ps on Cu at 2000 K (Yue, atoms per periodic cell).

$$\tau = \frac{\sum_i F_i p_i - \dot{\gamma}(t) \sum_i p_{xi} p_{yi}}{\sum_i p_i p_i}. \tag{15}$$

Thus, we assume isokinetic energy.

The shear viscosity $\eta(\dot{\gamma}, P, T)$ is defined as the ratio of the shear component of the stress tensor σ_{xy} and the applied shear rate $\dot{\gamma}$,

$$\eta(\gamma) = -\frac{\langle \sigma_{xy} \rangle}{\dot{\gamma}}. \tag{16}$$

Here

$$\sigma_{xy} = \frac{1}{\Omega} \left(\sum_{i=1}^{N} \frac{p_{xi} p_{yi}}{m_i} + W_{xy} \right), \tag{17}$$

where W_{xy} is the virial

$$W_{xy} = \frac{\partial U}{\partial \epsilon_{ij}}, \tag{18}$$

where ϵ is the strain tensor.

Our calculations lead to a square root dependence of viscosity on $\dot{\gamma}$ shear rate,

$$\eta(T, \rho) = \eta_0 + \eta_1 \sqrt{\dot{\gamma}} \tag{19}$$

(where the coefficients depend on temperature and density). Thus, we find nonNewtonian behavior. This square root relation was previously observed by Evans and Hanley [13, 14] for simple Lennard–Jones fluids examined under shear by NEMD.

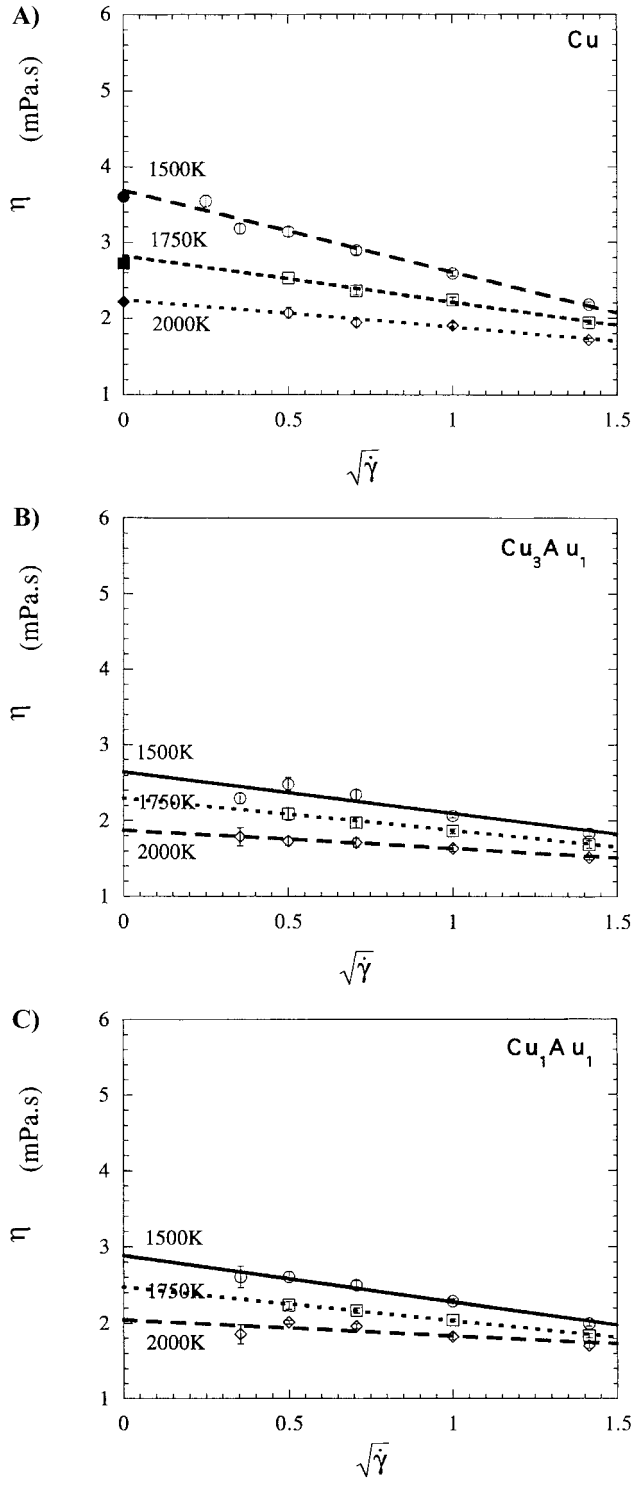

Figure 2. The calculated viscosities for various shear rates. (a) Cu. (b) Cu_3Au_1 ($x = 25\%$). (c) Cu_1Au_1 ($x = 50\%$). (d) Cu_1Au_3 ($x = 75\%$). (e) Au. The calculated values [open symbols (at $\gamma \neq 0$)] were based on three independent runs. The filled symbols (at $\gamma = 0$) are calculated from experiment [18] using the A and ΔG fitted to the experimental data. The lines are based on Eq. 19.

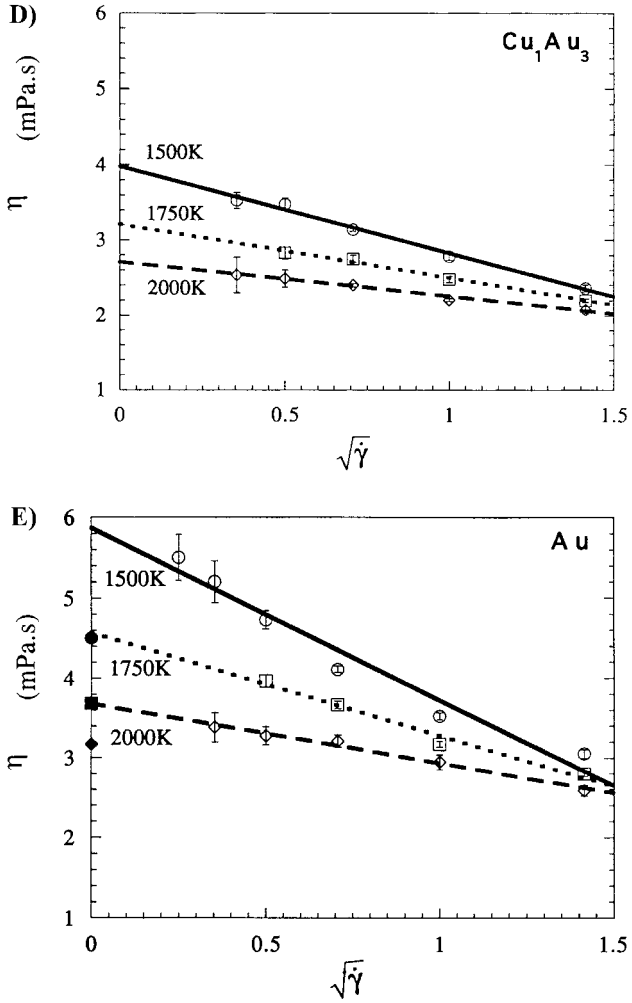

Figure 2. Continued.

Table 3. Simulation steps for various shear rates

Shear rate (1/ps)	2	1	0.5	0.25
N_{EQ}[a]	2000	4000	8000	16000
$N_{\text{total}} = N_{EQ} + N_{\text{meas}}$[b]	20000	40000	80000	160000

[a]Steps to equilibrate.
[b]Steps for measurement of properties.

2.3. METHOD

We considered simulation temperatures of 1500 K, 1750 K and 2000 K and for alloys $Au_x{-}Cu_{1-x}$ with $x = 0$, 0.25, 0.5, 0.75, and 1.0. The NEMD simulation was carried out in a cubic box (500 atoms per unit cell) subject to periodic boundary conditions. The unit cell length was based on extroplating the experimental density at the corresponding temperature [15]. For alloys we assume that the density is given by the linear combination rule

Table 4. Viscosity at zero shear rate, η_0 (mPas). The experimental data are calculated from fomular given by Ref. 18

T (K)	Cu		Cu_3Au_1	Cu_1Au_1	Cu_1Au_3	Au	
	Sim.	Exp.	Sim.	Sim.	Sim.	Sim.	Exp.
1500	3.68	3.6	2.64	2.88	3.97	5.86	4.5
1750	2.82	2.72	2.29	2.47	3.21	4.56	3.7
2000	2.24	2.22	1.87	2.04	2.70	3.67	3.2

Table 5. Temperature dependence of viscosity for Cu_xAu_{1-x} alloys (see Eq. 21)

		Cu	Cu_3Au_1	Cu_1Au_1	Cu_1Au_3	Au
ΔG (kcal/mol)	Simulation	24.15	16.56	16.05	18.78	23.69
	Calculated[a]	17.92	26.52	32.21	29.29	19.84
	Measured [19][b]	27.99	26.18	22.39	19.33	17.10
	Measured [18]	23.85				17.62
	Measured [17]	30.5				15.9
A (mPas)	Simulation	0.5298	0.7071	0.7711	0.8782	0.949
	Calculated[a]	0.740	0.5596	0.5623	0.5983	1.20
	Simulation [19][b]	0.3322	4222	0.6423	0.898	1.147
	Measured [18]	0.5287				1.099
	Measured [17]	0.3009				1.132

[a]Data came from results after density correction (Fig. 7b).
[b]Biscosities for alloy are extroplated from the experimental data at different compositions. (Figs. 6a and 7b).

$$\rho_T\,(Au_xCu_{1-x}) = \rho_T\,(Au)\,x + \rho_T\,(Cu)\,(1-x)\,. \tag{20}$$

The densities values we used are listed in Table 2.

To ensure that the system is equilibrated for the liquid state, we started with a random FCC alloy, raised the system to 300 K above the melting point, and equilibrated by constant temperature, constant volume (ThN) simulation, for 5ps (5000 steps of 1 fs) without shear (normal MD). This provided the starting structure for each NEMD simulation.

We considered applied shear rates of $\dot{\gamma} = 2$, 1, 0.5 and 0.25 (1/ps). For each shear rate and temperature, we first equilibrated (with NEMD) for N_{EQ} steps followed by $N_{\text{meas}} = 9N_{EQ}$ steps which were used to calculate properties. As the shear rate decreases we observed larger flucutations and slower convergence. Thus, we increased the number of steps. The total number of steps ranged from 20 000 ($\dot{\gamma} = 2$) to 100 000 ($\dot{\gamma} = 0.25$), as shown in Table 2. Figure 1 shows the convergence of the calculated viscosity for Cu at 2000 K.

We also partition each simulation into four segments to calculate a standard deviations for the viscosity. These results lead to the error bars shown in the figures; the largest deviation is less than 5% of the average viscosity.

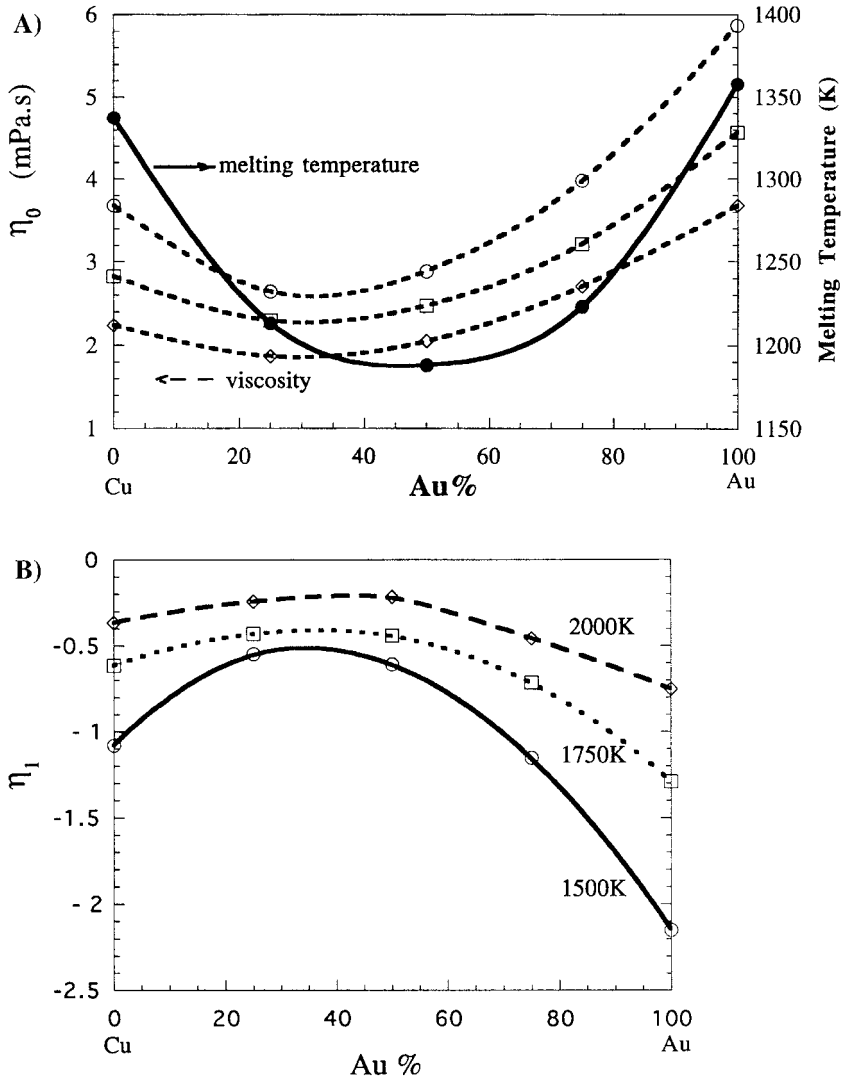

Figure 3. (a) The viscosity at zero shear rate (η_0) for Cu-Au alloys at various temperatures. (b) The non-Newtonian coefficient (η_1) in Eq. 19 for Cu-Au alloys at various temperatures.

3. Results and discussion

3.1. Comparison with experiment

The calculated viscosities for the various Cu_xAu_{1-x} alloys ($x = 0\%$, 25%, 50%, 75%, and 100%) are shown in Figure 2 for various shear rates and temperatures. This clearly shows the nonNewtonian behavior of liquid metals and alloys.

Fitting Eq. 19 to the calculations leads to the viscosities at zero shear rate, η_0 in Table 4. We find good agreement with experiment [18] for Cu (within 3.6%) and fair agreement for Au (within 14.6%). This may be because the FF parameters for Cu lead to a better description of the stacking faults and other properties than for Au or it may as well be due to the densities are inaccurate.

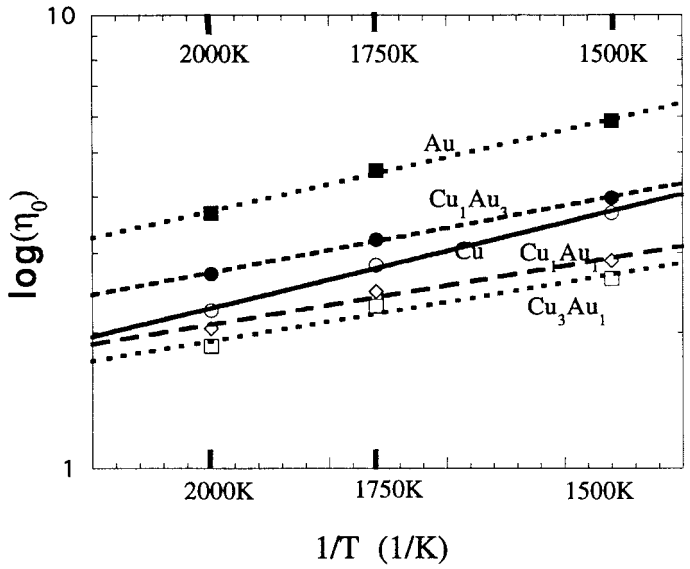

Figure 4. Viscosity of liquid Cu-Au alloys as a function of temperature.

3.2. TEMPERATURE DEPENDENCE

The η_0 and η_1 obtained for the alloys Cu_xAu_{1-x} are shown in Figure 3. The viscosity isotherm follows the trend of the liquidus and the density, as predicted by the Hirai estimation formula [1, 2]. The relation between $\ln(\eta)$ and $1/T$ is linear, as shown in Fig. 4. The viscosity in this region can be expressed as

$$\eta = A \exp\left(\frac{\Delta G}{RT}\right) \tag{21}$$

The values for A and ΔG are tabulated in Table 5 compared with the measured values from two references [17–19]. The energy of activation, ΔG, is a function of the composition of the melt.

To understand the origin of the temperature dependence, we considered the specific alloy Cu_1Au_3 and considered the dependence of viscosity on temperature, density, and structure. Figure 5a shows that starting with two different random FCC structures leads to an η_0 within 1.4%. This suggests that the precision in the calculated viscosity (using the same structure and density) is ~1.5%. We considered simulations using a fixed density (fixed at the value appropriate for 1750 K), but different temperatures (1500–2000 K). Figure 5b shows that the largest difference in η_0 is about 1.3%. *This indicates that η_0 depends only on density*; the dependence on temperature is only because of the change of density with temperature. Thus, using a fixed temperature and different densities (corresponding to 1500–2000 K) gives essentially the same η_0 as allowing the temperature and density to to readjust together. This shows that the dominant factor in determining the viscosity of liquid metals is the density! Thus, the variation of viscosity with temperature is caused by the variation in density with temperature. This implies that the dependence of viscosity of liquid metals on pressure can easily obtained from the temperature dependence at low pressure. Thus, to calculate the viscosity using NEMD we need to make sure to have the correct density at that temperature.

Figure 5 shows that the non-Newtonian coefficient, η_1, (viscosity as a function of shear rate) is almost independent of T and structure.

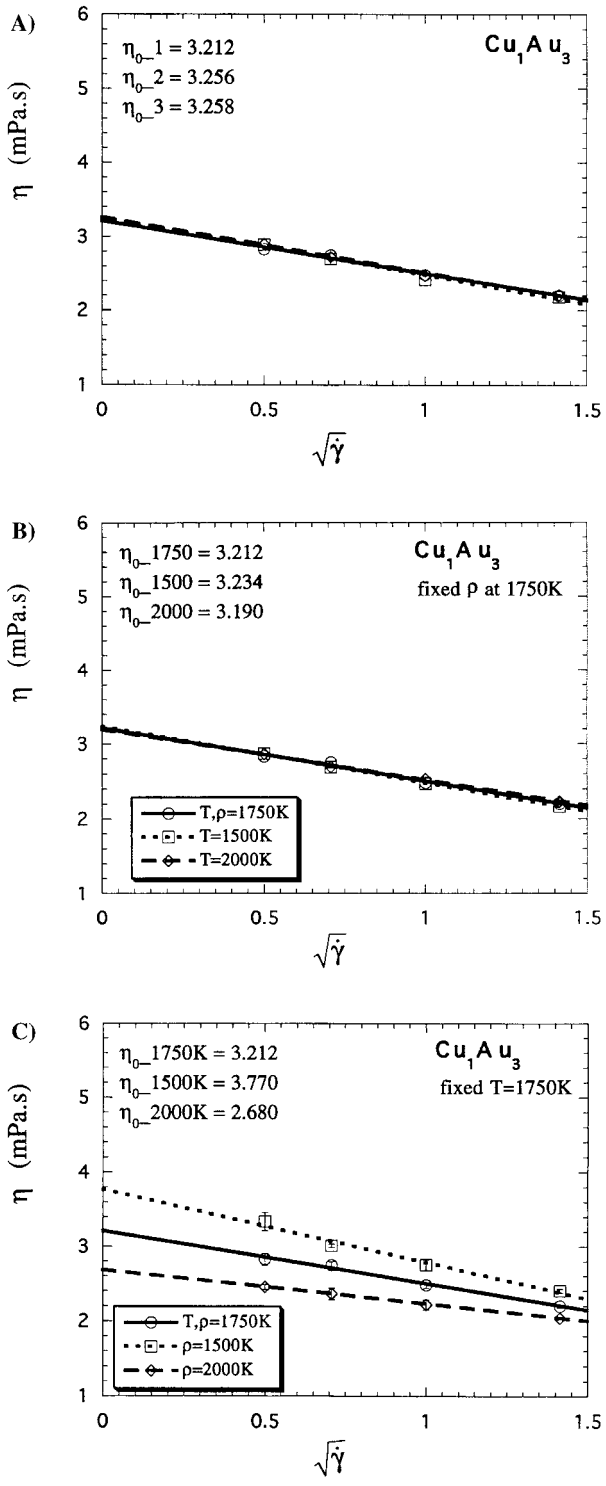

Figure 5. Viscosity of Au_3Cu_1. (a) Correct density for each simulation temperature, but starting from different random structures. (b) The density is kept fixed at the value of 1750 K, but the calculation temperature is varied. (c) The calculation temperature is fixed, but the density is varied among the value of that at 1500 K, 1750 K and 2000 K.

4. Summary

We calculated the viscosity of liquid Au-Cu alloys from NEMD simulations using the Q–SC many-body FF. The agreement with experimental viscosities of Cu at different temperature suggest that the NEMD and Q–SC can provide useful predictions.

We find that the temperature of the viscosity of liquid metal is determined by the density (and composition). We also find that the viscosity isotherm of the alloy follows the trend of the liqidus and the density curve.

Acknowledgements

This research was supported partially by a grant (ASCI-ASAP) from DOE, and grants (ARO-DAAH 95-1-0233) from the Army Research Office, from the NSF (ASC 92-17368 and CHE 95-12279). In addition, support for the Materials Simulation Center (MSC) facilities came from DOE-ASCI, ARO-DURIP (DAAG55-97-1-0140), Chevron Petroleum Technology Co., Asahi Chemical, Owens-Corning, Exxon, Asahi Glass, Nippon Steel, Avery Dennison, BP Chemical, and the Beckman Institute. Some calculations were carried out at the Illinois National Center for Supercomputing Applications (NCSA), funded by the National Science Foundation (NSF).

References

1. Hirai, M., Iron Steel Inst. Japan Int., 33 (1993) 251.
2. Seetharaman, S. and Sichen, D., Iron Stell Inst. Japan Int., 37 (1997) 109.
3. Heyes, D.M., Comp. Phys. R., 8 (1988) 71.
4. Evans, D.J. and Morriss, G.P., Statistical Mechanics of Nonequilibrium Liquid, Academic Press, London, 1990.
5. Koishi, T., Arai, Y., Shirakawa, Y. and Tamaki, S., J. Phys. Soc. Japan, 66 (1997) 3188.
6. Mundy, J., Balasubramanian, S., Bagchi, K., Siepmann, J.I. and Klein, M.L., Faraday Discussions, 104 (1996) 17.
7. Allen, W. and Rowley, R.L., J. Chem. Phys.,106 (1997) 10273.
8. Balasubramanian, S., Mundy, C.J. and Klein, M.L., J. Chem. Phys., 105 (1996) 11190.
9. Sarman, S., Cummings, P.T. and Evans, D.J., Intl. J. Thermophysics, 15 (1994) 1125.
10. Sutton, A.P. and Chen, J., Phil. Mag. Lett., 61 (1990) 139.
11. Rafii-Tabar, H. and Sutton, A.P., Phil. Mag. Lett., 63 (1991) 217.
12. Kimura, Y., Cagin, T. and Goddard, W.A. III, unpublished; Cagin, T., Qi, Y., Li, H., Kimura, Y., Ikeda, H., Johnson, W.L., Goddard, W.A., III in Bulk Metallic Glasses, MRS Symp. Series Vol. 554, 43–48 (1999), Inoue, A., Johnson, W.L., Liu, C.T. (eds.)
13. Evans, J., Phys. Lett., A74 (1970) 229.
14. Evans, J. and Hanley, H.J.M., Phys. Rev., A20 (1979) 1648.
15. Handbook of Chemistry & Physics, 51st edition, Chemical Rubber Co., 1971.
16. Handbook of Chemistry & Physics, 74th edition, CRC Press, New York, 1991.
17. Smithells Metals Reference Book, 6th editon, Butterworths Co., 1983.
18. Handbook of Physico-Chemical Properties at High Temperatures, The 140th Committee of Japan Society for Promotion of Science, ISIJ, Tokyo, 1988.
19. Gebhardt, E. and Worwag, G., Z. Metallkunde, 42 (1951) 358.